IPA18-125-SG

PROCEEDINGS, INDONESIAN PETROLEUM ASSOCIATION
Forty-second Annual Convention, May 2018

LITHOLOGY DISCRIMINATION AND PORE-FLUID DETECTION USING 3D PRE-STACK SIMULTANEOUS INVERSION: A CASE STUDY AT GUMAI FORMATION, JAMBI SUB-BASIN, SOUTH SUMATRA.

Widia Anggraeni*
Mawar Indah Nursina**
Andri Syafriya**
Bagus Sapto Mulyatno*
Muh Sarkowi*

ABSTRACT

Pre-stack simultaneous inversion is a part of quantitative interpretation as a reservoir characterization tool to identify lithology and pore fluid based on P-wave velocity, S-wave velocity, and density. The Gumai Formation facies architecture is complex and formed by interbedded sand and – shale. The formation has various roles in the Jambi Sub-Basin petroleum system acting as the regional seal, source rock, and reservoir rock. This research was carried out in order to discriminate lithology and detecting pore fluid distribution using Pre-stack Simultaneous Inversion in the Gumai Formation, Jambi sub-basin which is supported by the proven discoveries of hydrocarbon (gas) while Drill Stem Testing (DST). The data consists of 3D seismic partial-angle stacks and well log data which are used as input to three-term Fatti equation to transform the seismic trace into reflectivity. Further, reflectivity from different angle stacks are simultaneously inverted to obtain P-impedance (Zp), S-Impedance (Zs) and Density (ρ). The simultaneous inversion results for gas bearing sand reservoir encased in shale gave low P-Impedance value (15,700-18,250 ft/s*gr/cc or 4,785-5,563 m/s*gr/cc), low S-Impedance value (9,078-10,850 ft/s*gr/cc or 2,767-3,307 m/s*gr/cc) and low density value (2.10-2.19 gr/cc). Based on these values, combined maps of P-impedance (Zp), S-Impedance (Zs) and Density (ρ) show the distribution of the prospective areas for gas bearing sand reservoir towards western part of the study area.

keywords: seismic, simultaneous inversion, Gumai Formation, gas reservoir

INTRODUCTION

The South Sumatera basin has been a prolific hydrocarbon producing basin in Indonesia since the first discoveries of the surface seep at Kampung Minyak Field in 1886 (Macgregor, 1995 after Bishop, 2001). Based on the USGS World Energy Assesment Team (2000), it is estimated that South Sumatra Basin has the potential of undiscovered conventional oil, gas, and condensate are 469 million barrels of oil (MMBO), 18,250 billion cubic feet of gas (BCFG), and 239 million barrels of natural gas liquids (MMBNGL), in the South Sumatra assesment unit or 3.7 BBOE by the year 2025.

South Sumatera basin has several sub-basins, one of them is Jambi sub-basin, with the Gumai Formation as primary target. The Gumai Formation was formed during maximum phase of transgression in the Early Miocene to Middle Miocene, and comprises predominantly deposits of interbedded marine shales, sandstone, and siltstone. The Gumai Formation has various roles in the Jambi sub-basin petroleum system acting as regional seals, source rock, and potential sand reservoir. A stratigraphic chart of Jambi sub-basin is shown in Figure 1. The widespread marine shales of the Gumai Formation act as the regional seal and provides the highest quality seal for the Upper Talang Akar, Batu Raja equivalent and Gumai Formation (Ginger and Fielding, 2005). Additionally, Gumai Formation also plays the role as source rocks where Gumai shales have TOC 0.71-8.00 with a Hydrogen Index (HI) ranging from 34-603, that shows the formation as oil and gas prone (Marpaung et al, 2006). Finally, the Gumai reservoir potential in this area has been proven by the discoveries of hydrocarbon (gas) while drill stem testing (DST).

***   University of Lampung**
****   PetroChina International Jabung Ltd**

A Previous study by Nursina et al. (2017) characterized the Gumai Formation using acoustic impedance (or P-Impedance) generated from Simulated Annealing Inversion in order to determine reservoir distribution more clearly.

The difficulty discriminating the lenticular sand bodies and pore fluid in the shaly sand of the Gumai Formation requires quantitative interpretation techniques as reservoir characterization tools that can provide reliable estimates of P-wave velocity, S-wave velocity, density or Poisson's ratio information. The common goal of these methods is to extract information about lithology, reservoir quality, and pore fluids from pre-stack seismic amplitudes (Chopra & Castagna, 2014). Therefore, pre-stack simultaneous inversion was chosen to be applied for this study.

METHODS

Pre-stack simultaneous inversion was performed to compute P-Impedance and S-Impedance from the pre-stack gather seismic data (Chopra and Castagna, 2014). This can ultimately be used to generate lithology and fluid properties (Bailey et al, 2010).

Aki and Richards (1980) derived an approximation to the Zoeppritz equation for the reflection compressional wave in a form that comprises three terms; density, P-wave velocity, and S-wave velocity. The equation reads as follows:

$$R(\theta) = a\frac{\Delta\rho}{\rho} + b\frac{\Delta\alpha}{\alpha} + +c\frac{\Delta\beta}{\beta}$$

Fatti et al. (1994) rearranged an approximation to the Aki and Richards approximation which is given as:

$$R_{pp}(\theta) = c_1 R_{P0} + c_2 R_{S0} + c_3 R_D$$

Where Rpp(θ) is angle-dependent reflectivity, R_{P0} is zero-offset P-reflectivity, R_{S0} is zero-offset S-reflectivity, R_D is the density reflectivity, and:

$$c_1 = 1 + \tan^2\theta$$

$$c_2 = -8\left(\frac{Vs}{Vp}\right)^2 \tan^2\theta$$

$$c_3 = -\frac{1}{2}\tan^2\theta + 2\left(\frac{Vs}{Vp}\right)^2 \sin^2\theta$$

The simultaneous inversion is performed based on the Fatti et al. equation (1994) using the reflectivity to extract estimations of the P-impedance, S-impedance, and density from the pre-stack seismic gathers. Hampson et al. (2005) extended the work of Simmons and Backus (1996) and Buland Omre (2003), and developed a new approach that yields P-impedance, S-impedance, and density as inversion products (Chopra and Castagna, 2014).
The pre-stack simultaneous inversion workflow is shown in Figure 2. The datasets used in this study consist of 3D seismic partial angle stacks - divided into three parts, near angle stack (4^o-18^o), mid angle stack (18^o -32^o) and far angle stack (32^o-47^o), well log data (TR-1, TR-3, TR-4, and TR-6), and horizon interpretation.

The workflow starts with seismic and well log data conditioning prior to the inversion process. Simultaneous Inversion requires wavelet for each angle stacks. In this study, wavelet extraction is performed using statistical wavelet. The second step, shear wave log prediction, is performed because of the limited amount of shear wave data is available (from the 4 wells only 1 well has shear wave information). Shear wave log prediction was performed using Fluid Replacement Modelling (FRM) with reservoir properties as input (saturation water, hydrocarbon saturation, volume clay) and calibrated using TR-3 measured shear wave log. Thirdly, the well ties to the seismic volume to maximize the correlation between measured and synthetic data. Then, initial model was built using low-frequency model, constrained by the horizon, seismic RMS velocity, and partial angle wavelets as the input for the inversion. After that, pre-inversion analysis is conducted to control the quality of the inversion result based on the algorithm to minimize the error between the model and measured data. Finally, the pre-stack simultaneous inversion based on three-terms Fatti equation was used to invert the partial angle stacks into P-impedance, S-impedance, and Density.

RESULTS

The target zone of this study is the sandstone reservoir in Gumai Formation, which has potential hydrocarbon (gas) validated by the Drill Stem Test data (DST) at a depth of 3,274 ft (998 m) – 3,290 ft (1003 m) on the key well TR-1. The seismic section is shown in Figure 3 with target zone marked by black oval. The full-stack seismic (left side) exhibits the appearance of the bright spots around 1,100 ms two-way-time (TWT). On the right side, the seismic partial angle stacks (near, mid and far) show the amplitude increasing to the far angle and is commonly called the AVO anomaly which infers direct hydrocarbon indicator (DHI).

In order to discriminate the lithology and pore fluid, the inversion result will be compared with the cross-plot of well log data. The lithology sensitivity shown in Figure 4 cross-plotted P-impedance versus shear impedance log and is coloured-coded by gamma-ray log. This clearly distinguishes between sand and shale, where sand is indicated by low gamma-ray value less than 70 API, low P-impedance with cut-off value 18,400 (ft/s*gr/cc) or 5608 (m/s*gr/cc), and low shear impedance value 10,200 (ft/s*gr/cc) or 3,109 (m/s*gr/cc) showed low impedance sand as opposed to surrounding shales. The next parameter indicator regarding the pore fluid is Vp/Vs ratio. Tatham (1982) mentioned the Vp/Vs ratio is especially sensitive to the pore fluid found in sedimentary rocks. Based on Goodway (2001) the Vp/Vs ratio value of 1.71 (unitless) is classified as gas sand and Vp/Vs ratio for shales has a value of 2.25 (unitless) (Vp/Vs ratio average change is 27%). The calculation of Vp/Vs ratio (Table 1) on the target zone gives an average value of 1.85 (unitless) which indicates a gas sand affected by surrounding shale due to the geological condition of Gumai shaly sand.

The inversion results for the P-Impedance (Zp), S-Impedance (Zs) and density (ρ) on Figure 5 (yellow highlighted) demonstrates a good matching correlation curve between inverted data compared to the well log (measured data). The results are presented in the horizon slice map overlaid within the time structure contour map in the study area. Figure 6 shows the distribution of P-impedance (Zp), where the target zone is interpreted as low impedance with values ranging from 15,700-18,250 (ft/s*gr/cc) or 4,785-5,563 (m/s*gr/cc) which is shown in red to yellow colour and delineated by black oval. The second inversion result is S-impedance (Zs) shown in Figure 7, where the target zone is interpreted as low impedance with values ranging from 9,078-10,850 (ft/s*gr/cc) or 2,767-3,307 (m/s*gr/cc) which is shown in red to yellow colour and delineated by a black oval. The low impedance value closely relates to rocks with high porosity. The third result is the density (ρ) shown in Figures 8. The target zone is identified as low density with the values ranging from 2.10 – 2.19 (gr/cc). This is interpreted as sandstone with a density value lower than surrounding shale. Based on Chopra and Castagna (2014) the density of gas sand reservoir drops more rapidly than oil sand reservoir.

In addition, the comparison of the P-Impedance (Zp) and S-Impedance (Zs) values from the inversion result with the well log value at the well location showed a good match. Also, the result of the density and Vp/Vs ratio was interpreted as gas-filled sandstone with the delineation of prospect zone towards the west of study area.

CONCLUSIONS

The application of pre-stack simultaneous inversion in Gumai Formation has been proven to discriminate the lithology and pore fluid based on the low P-Impedance (Zp), low shear impedance (Zs), and low density (ρ) which are interpreted as gas-filled sandstones with the distribution of the prospect zone towards the west of study area. These results can be used for further planning of exploration in the Gumai Formation, Jambi Sub-basin, South Sumatra.

ACKNOWLEDGEMENTS

We would like to thank PetroChina International Jabung Ltd., for providing the data used in this study.

REFERENCES

Aki, K. and Richards, P.G., 1980, Quantitative Seismology, Theory and Methods: W.H. Freeman & Co.

Bailey, Brad. Barclay, F. Nesbit, R. and Paxton A., 2010, Prospect Identification using Inversion and Lithology Prediction, Expanded Abstract of Australia SEG Annual Meeting p.1-4.

Buland, A. and Omre, H., 2003, Bayesian Linearized AVO Inversion: Geophysics, v.68, p.185-198.

Chopra, Satinder and Castagna J. P., 2014, AVO: Society of Exploration Geophysicist.

Fatti, J., Smith, G., Vail, P., Strauss, P., and Levitt, P., 1994, Detection of Gas in Sandstone Reservoirs Using AVO analysis: a 3D Seismic Case History Using the Geostack Technique: Geophysics, v.59, p.1362-1376.

Ginger D., and Fielding K., 2005, The Petroleum System and Future Potential of The South Sumatra Basin: Proceeding of Indonesian Petroleum Association.

Goodway, Bill., 2001, AVO and Lamé Constants for Rock Parameterization and Fluid Detection: CSEG Recorder, v.26, p.39–60.

Hampson, D., Russell, B., and Bankhead, B., 2005, Simultaneous Inversion of Pre-Stack Seismic Data: CSEG National Convention, p.1-4.

Marpaung, L P., Dono H M., Satyana, A H., and Eddy, A S., 2006, Oil Family Characterisation of Jabung Area, Jambi Sub-Basin: Proceedings Joint Convention Surabaya 2005 – HAGI-IAGI-Perhapi.

Macgregor, D. S., 1995, The exploration significance of surface oil seepage: an Indonesian perspective: Proceedings Indonesian Petroleum Association Twenty-fourth Annual Convention, October, 1995, p. 97-109., In Bishop G, Michele., 2001, South Sumatra Basin Province, Indonesia: The Lahat/Talang Akar-Cenozoic Total Petroleum System: Open-File Report 99-50-S. USGS.

Nursina, I M., Wibawa, I.G A surya., Badri M A., and Siregar, R D., 2017, Upside Potential Reservoir Characterization Using Simulated Annealing Inversion to Optimize Reservoir Performance in Shale Dominant Gumai Formation-Jabung Block: Proceeding of Joint Convention Malang HAGI-IAGI-IAFMI, IATMI.

Simmons, J.L., dan Backus, M.M., 1996, Waveform-based AVO Inversion and AVO Prediction-Error: Geophysics, v.61, p.1575-1588.

Suta, I Nyoman., 2003, Reservoir Characterization of Lower Talang Akar Fluvial Sandstone Northeast Betara (NEB) Field, South Sumatera Basin, Indonesia: A Thesis - University of Oklahoma.

Tatham, H Robert., 1982, Vp/Vs and lithology: Geophysics, v.47, p.336–344.

U. S. Geological Survey World Energy Assessment Team, 2000, U. S. Geological Survey World Energy Petroleum Assessment 2000-Description and Results: USGS Digital Data Series DDS-60, four CD-ROMs., In Bishop G, Michele., 2001, South Sumatra Basin Province, Indonesia: The Lahat/Talang Akar-Cenozoic Total Petroleum System: Open-File Report 99-50-S. USGS.

TABLE 1

THE CALCULATION OF VP/VS RATIO ON THE TARGET ZONE AT WELL TR-1 WITH 6 SAMPLES

sample	**1**	**2**	**3**	**4**	**5**	**6**
Vp (ft/s)	7814	7977	8033	8161	8363	8447
Vs (ft/s)	4256	4320	4363	4452	4476	4549
Vp/Vs ratio	1.84	1.85	1.84	1.83	1.87	1.86
Vp/Vs ratio average						**1.85**

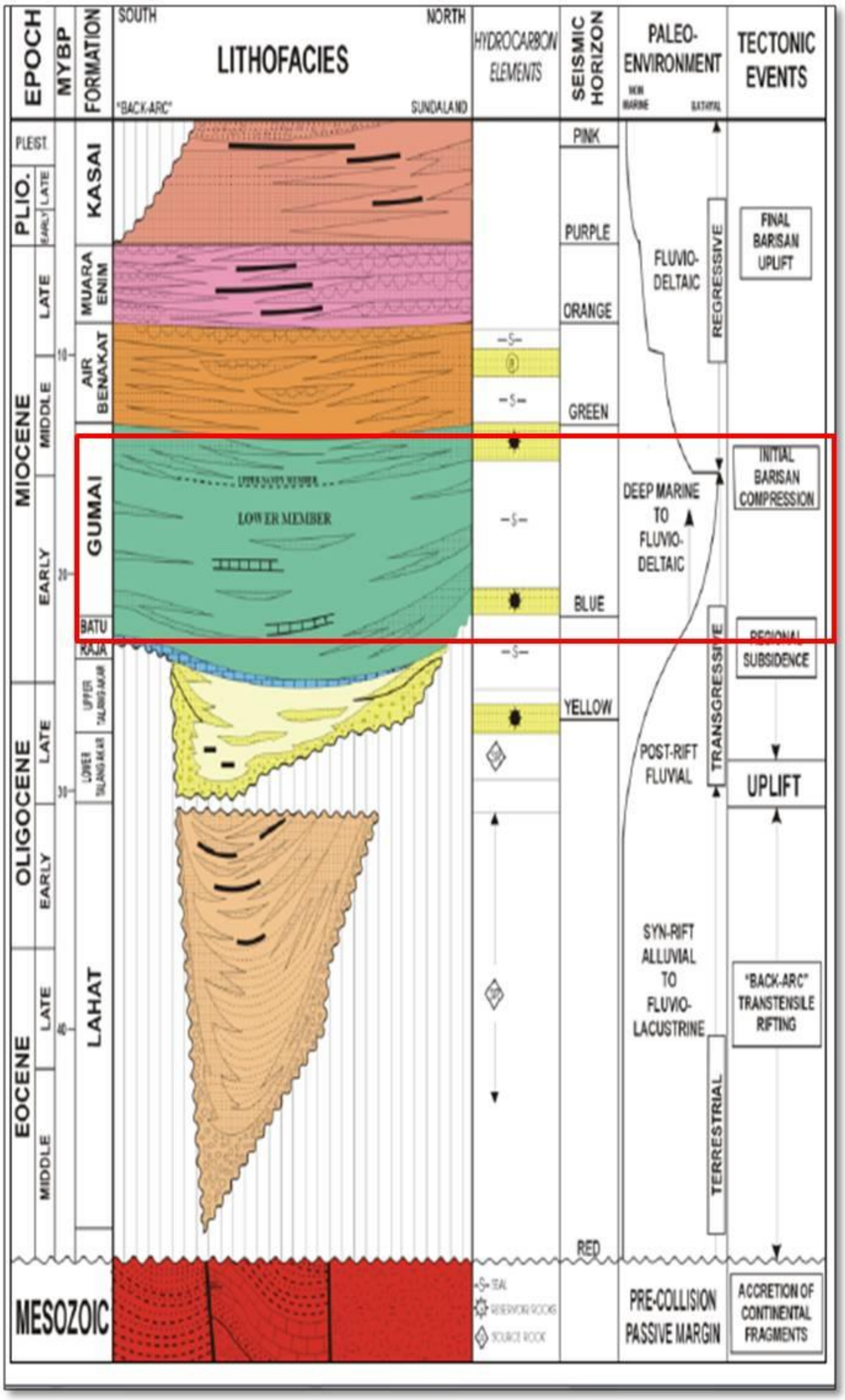

Figure 1 - The Stratigraphy Chart of Jambi Sub-basin, Red rectangle shows the study focused on Gumai Formation (Suta, 2003).

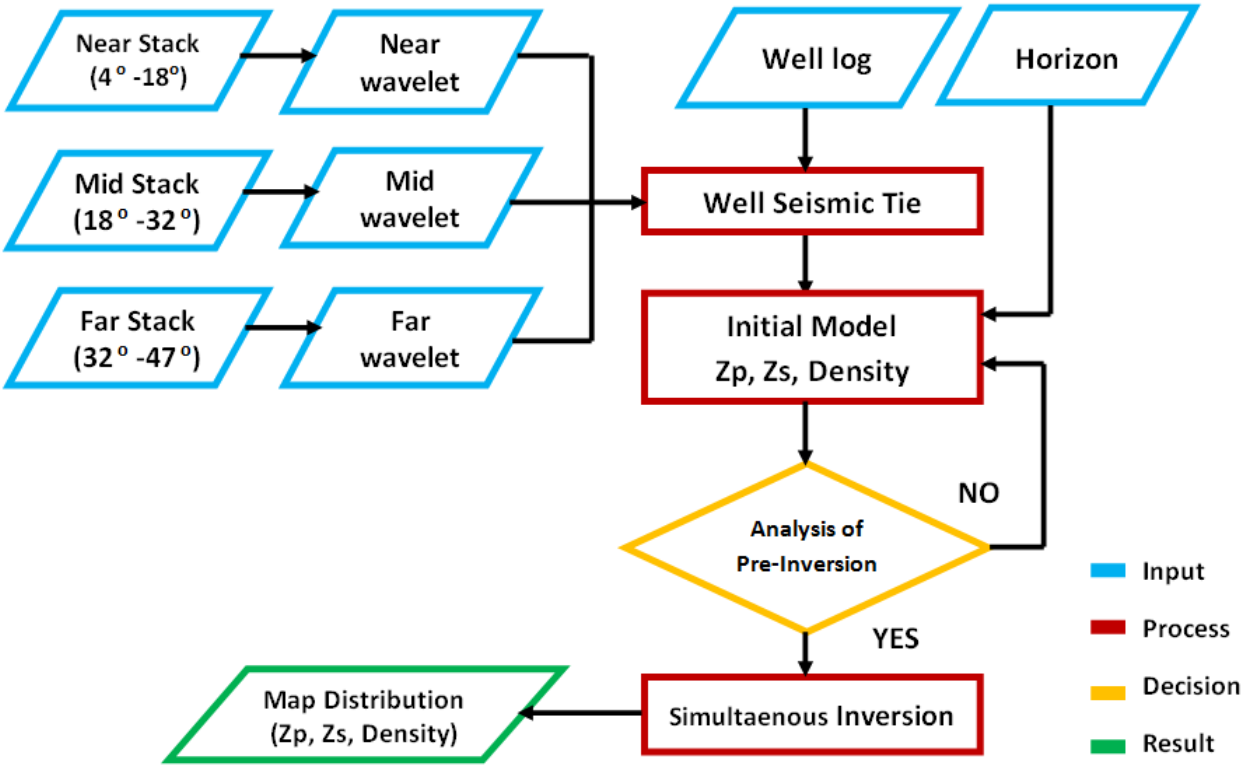

Figure 2 - The workflow of Pre-stack Simultaneous Inversion – used to invert seismic partial angle stack to yield the P-impedance, S-impedance, and Density.

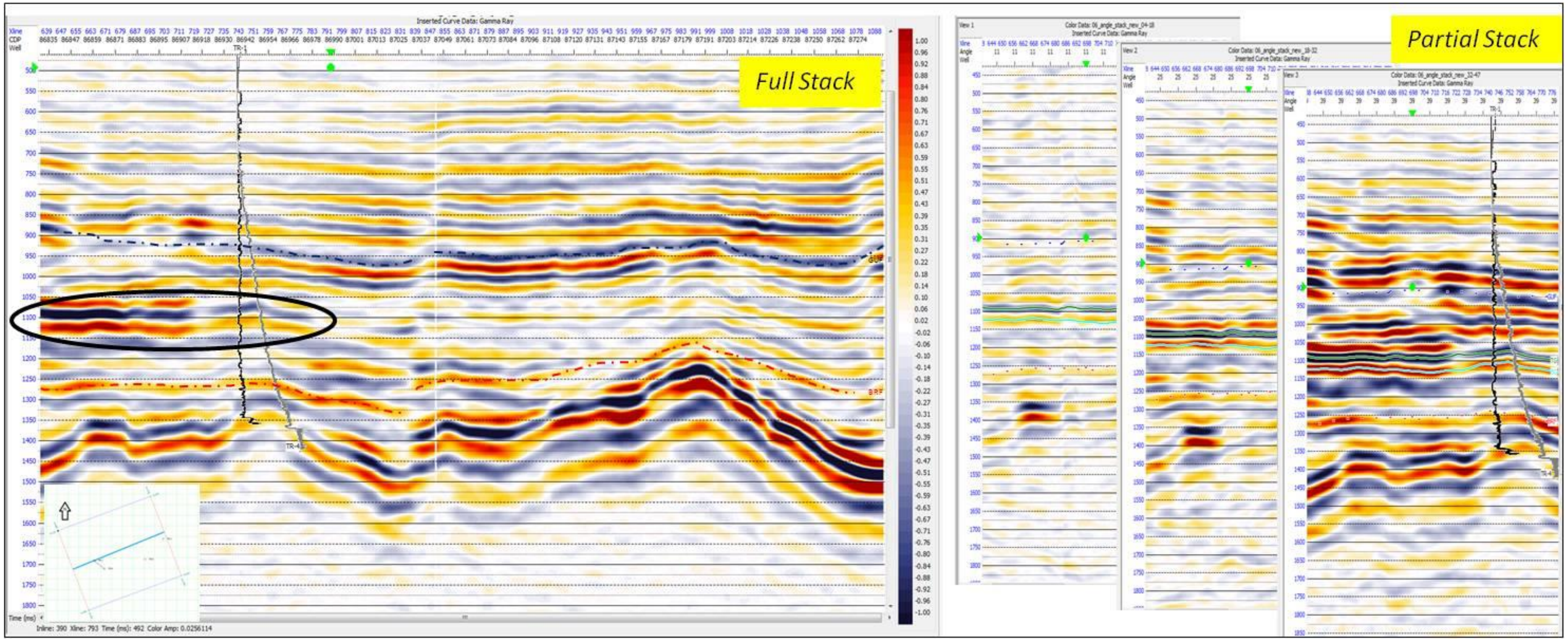

Figure 3 - The left side is the full stack seismic shown the target on the bright spots zone (black oval) and the right side is the seismic partial angle stack (in degrees, near 4-18, mid 18-32 and far 32-47) which shows the amplitude increasing to the far angle, is commonly called as the AVO anomaly used for direct hydrocarbon indicator (DHI).

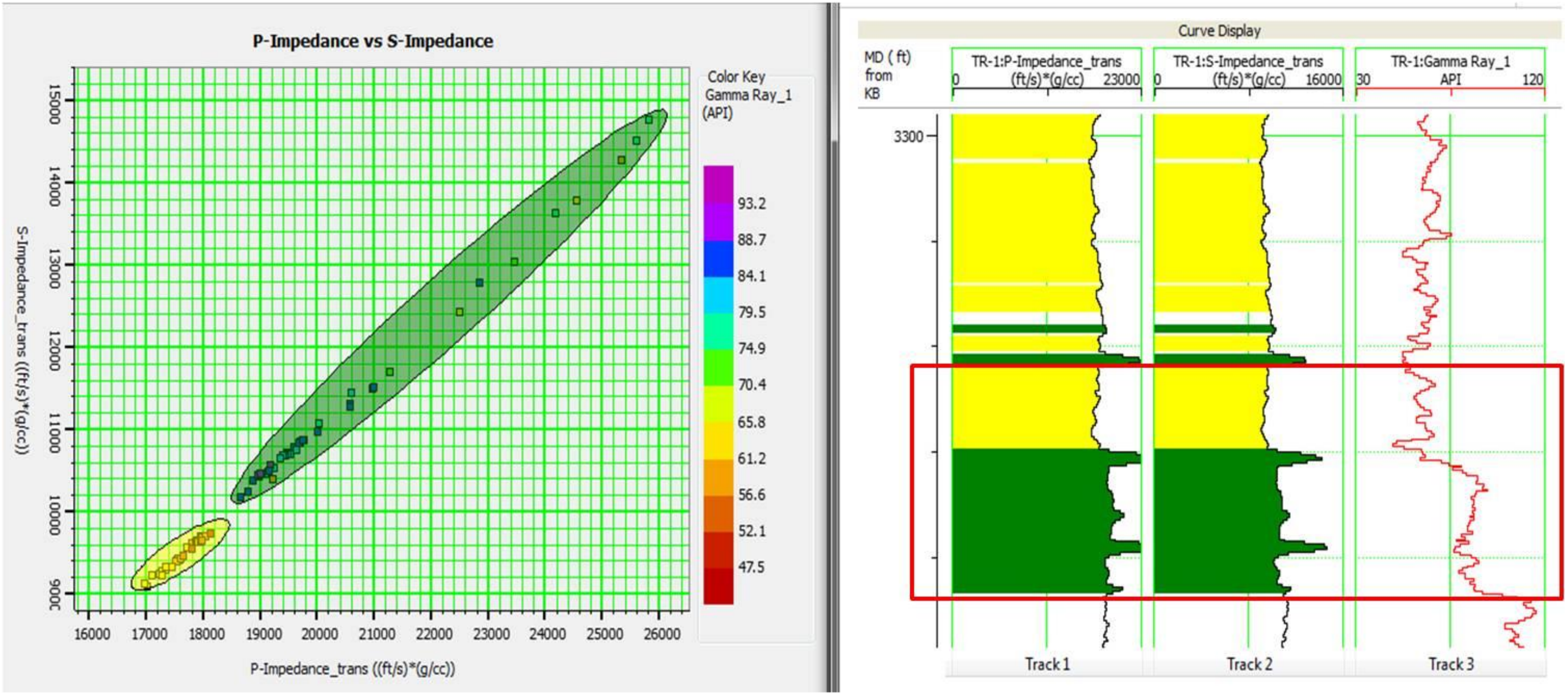

Figure 4 - Lithology sensitivity on the well TR-1, left side: cross-plotted P-impedance log versus S-impedance log coloured-coded by gamma ray, which clearly distinguishes between the sandstone (yellow oval zonation) with lower impedance and shales with higher impedance (green oval zonation). The right side demonstrates the cross-section on the log based on coloured zonation, which target zone (yellow colour) shows low impedance and low gamma-ray.

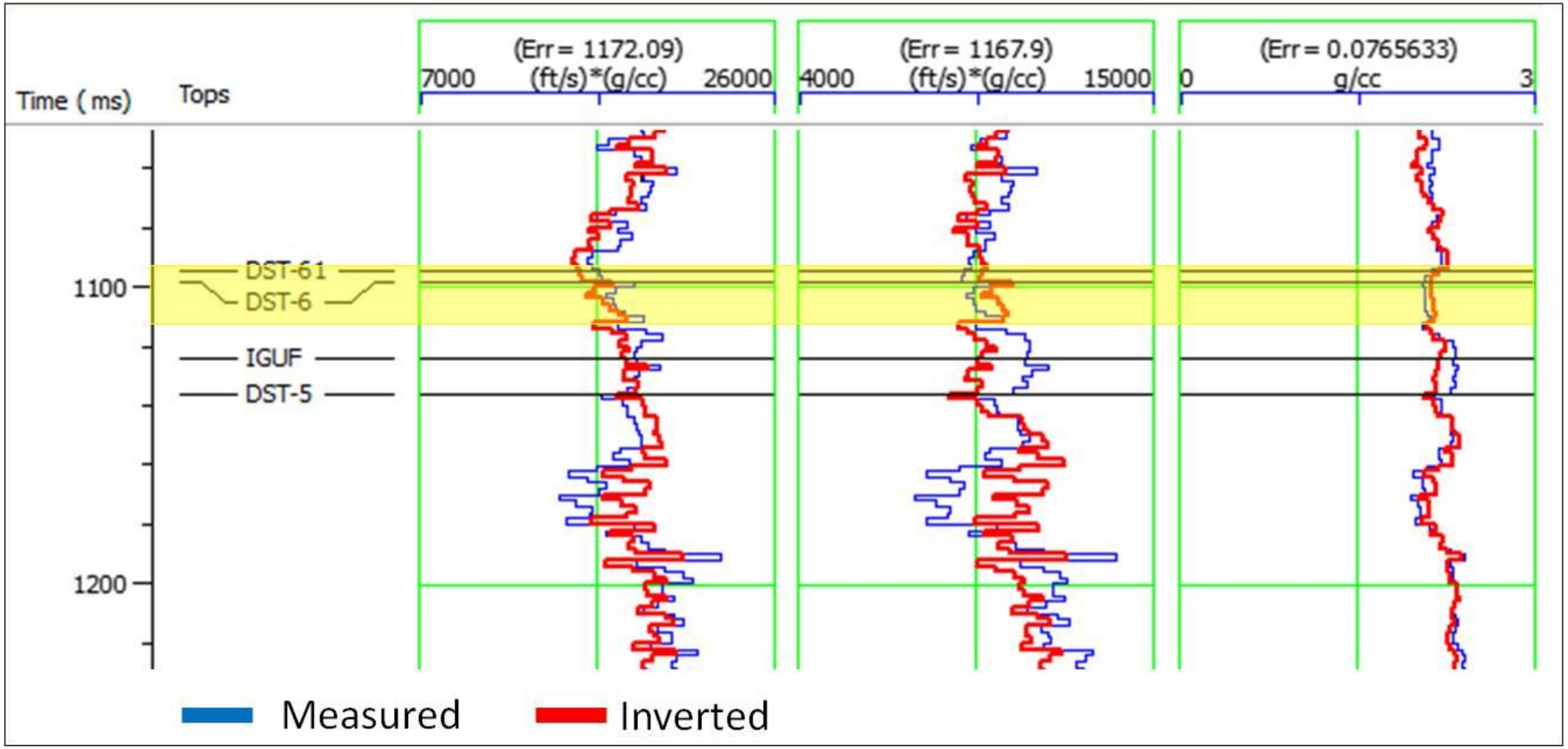

Figure 5 - Inversion analysis, P-impedance (left side), S-impedance (middle), and density (right side) on the well TR-1. The inversion result for P-impedance, S-impedance and density was in good match curve between inverted result data and the well log (measured data).

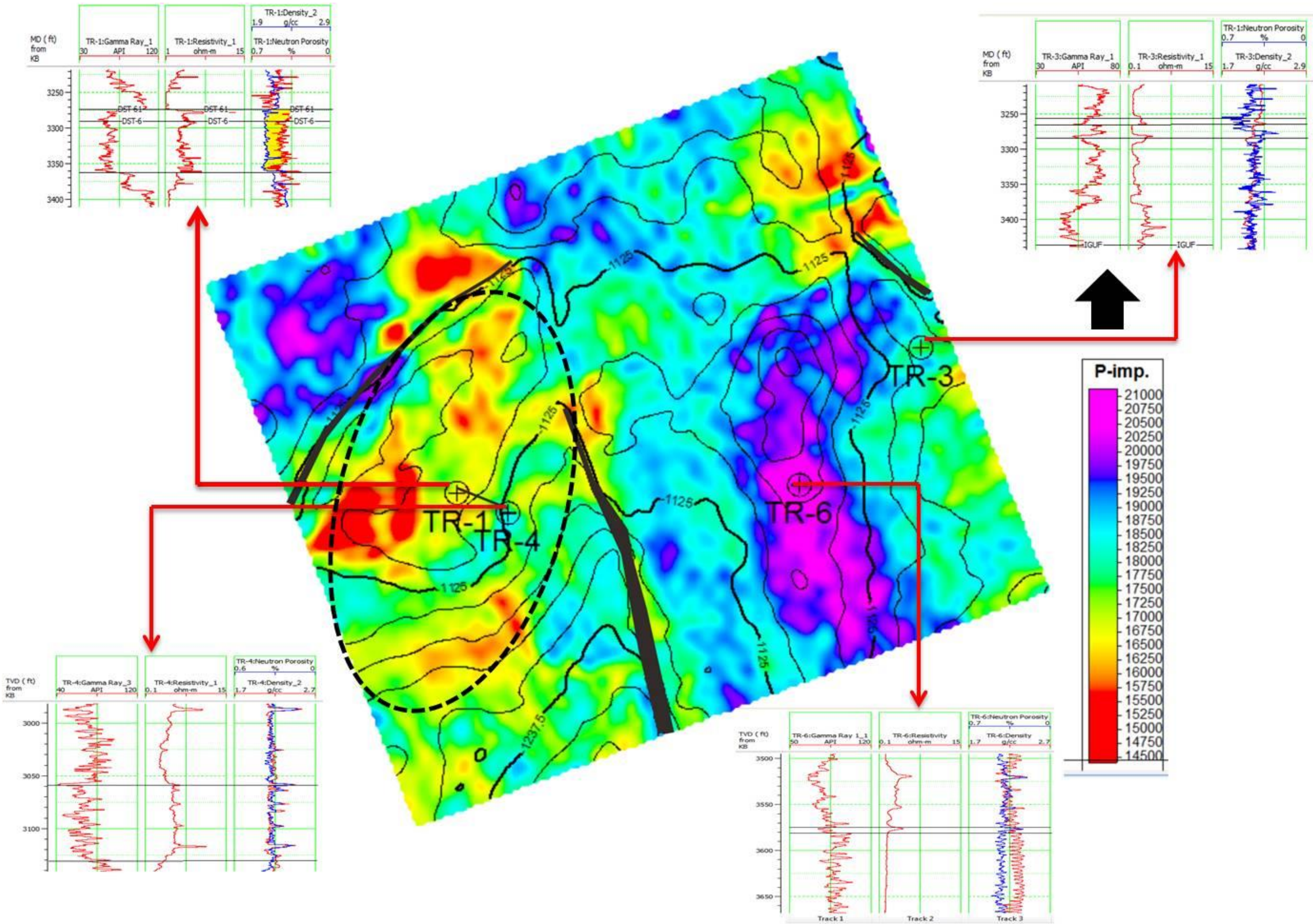

Figure 6 - The map distribution of P-impedance inversion result overlaid with time structure map (contour interval is 22.5 ms), which shows low P-impedance value (red to yellow colour) as the gas sand reservoir that delineated by a black oval in the west direction. The four wells trajectories and log parameters (gamma ray, resistivity, density, and neutron porosity) are shown.

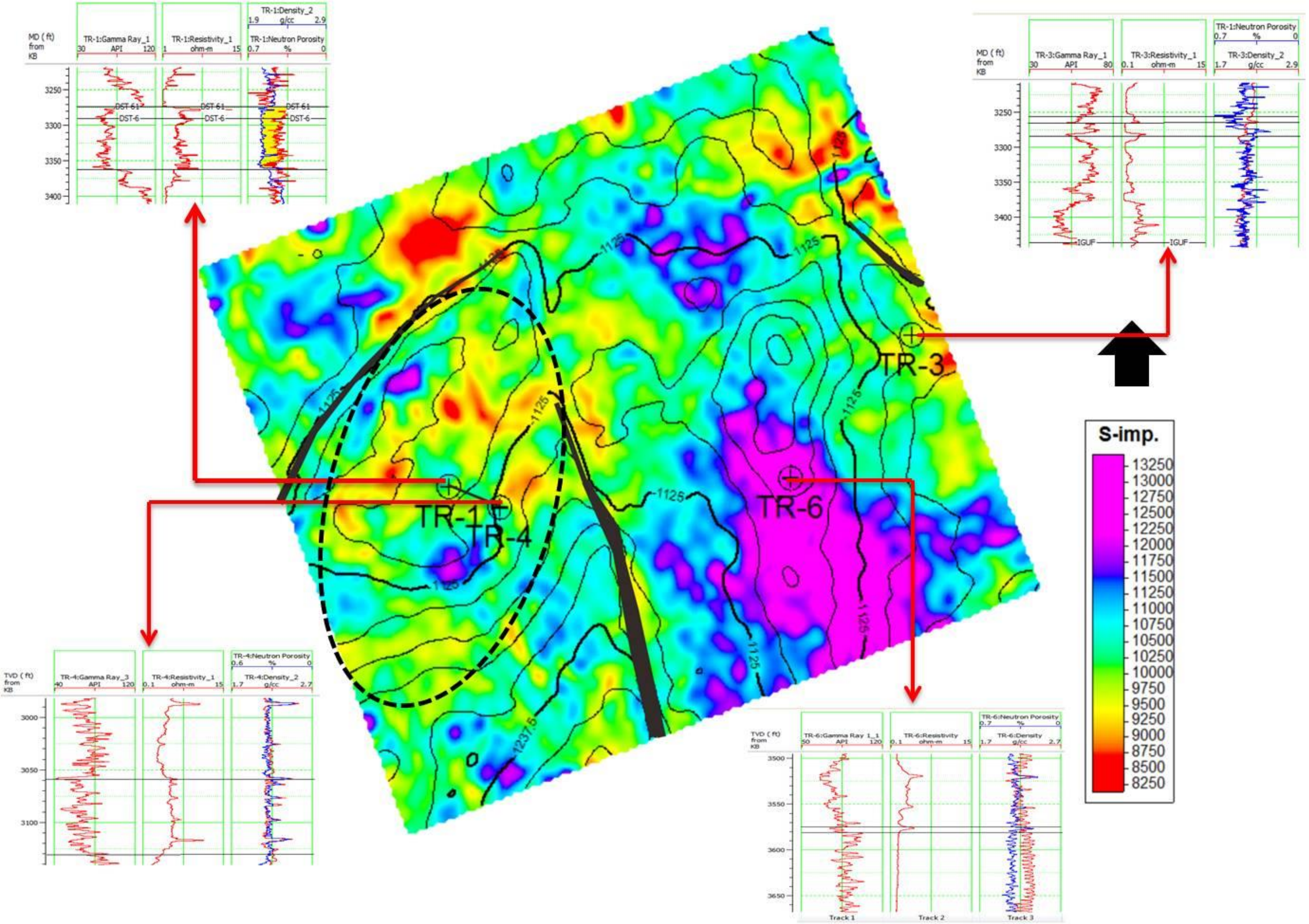

Figure 7 - The map distribution of S-impedance inversion result overlaid with time structure map (contour interval is 22.5 ms), which shows low S-impedance value (red to yellow colour) as the gas sand reservoir that delineated by a black oval in the west direction. The four wells trajectories and log parameters (gamma ray, resistivity, density, and neutron porosity) are shown.

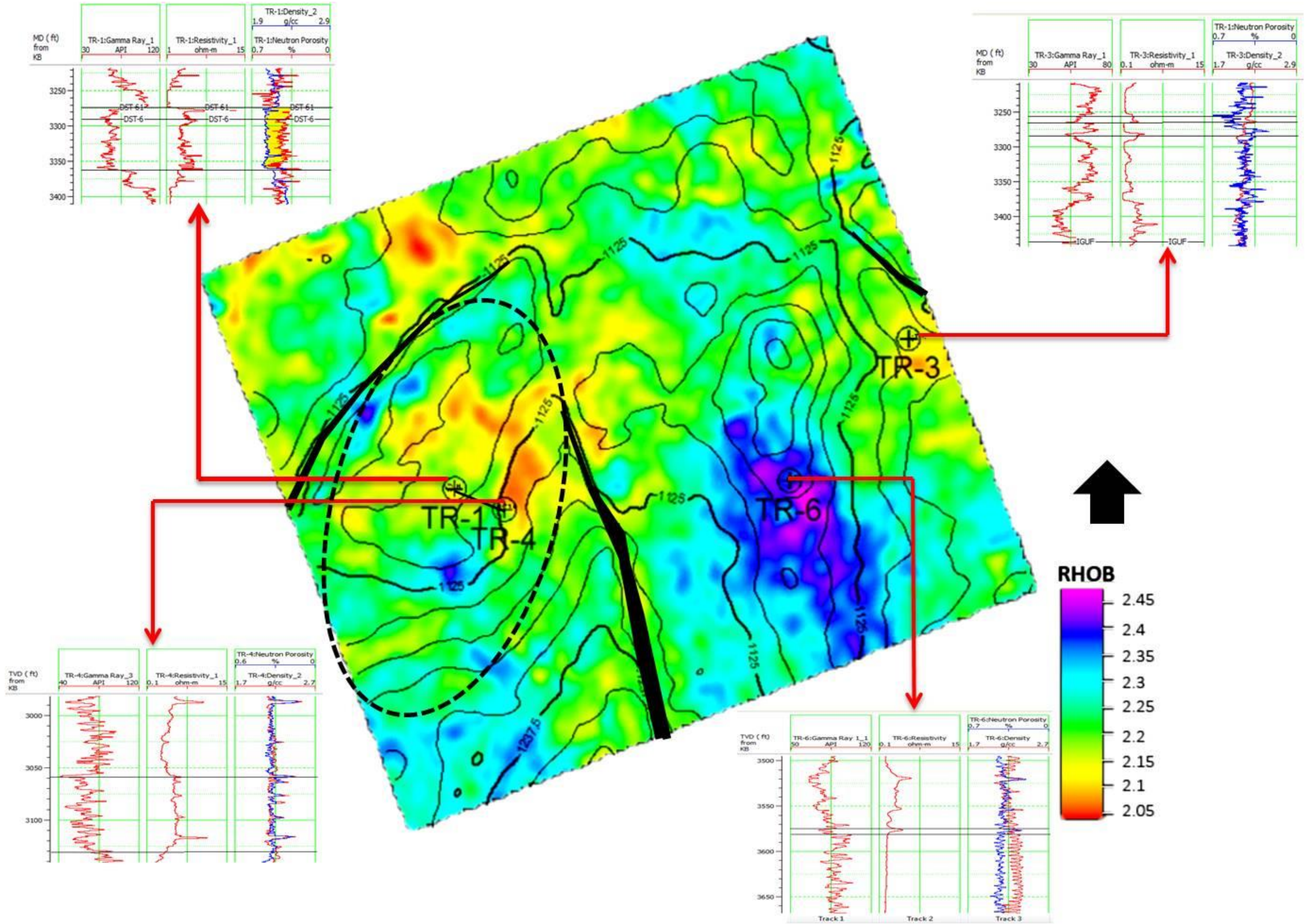

Figure 8 - The map distribution of density (ρ) inversion result overlaid with time structure map (contour interval is 22.5 ms), which shown low density value (red to yellow colour). Interpretatation of the gas sandstone reservoir has lower density than surrounding shales, that delineated by a black oval in the west direction. The four wells trajectories and log parameters (gamma ray, resistivity, density, and neutron porosity) are shown.